Jour. Geol. Soc. India (2022) 98:471-478
https://doi.org/10.1007/s12594-022-2004-3

ORIGINAL ARTICLE

Seismic Site Characterization Using Ambient Noise and Earthquake HVSR in the Easternmost Part of Shillong Plateau, India

Athira Vijayan, Mohit Agrawal* and Ravindra K. Gupta

Department of Applied Geophysics, Indian Institute of Technology (Indian School of Mines), Dhanbad - 826 004, India.
***E-mail:** mohit@iitism.ac.in*

Received: 3 June 2021 / Revised form Accepted: 4 October 2021

ABSTRACT

This study provides site characterization results using passive seismic techniques for the easternmost part of Shillong plateau of Northeastern India. The prime objective of this research is to generate the Horizontal-to-Vertical Spectral Ratios (HVSR) from earthquakes and ambient microtremor data for generation of 1-D shear wave velocity profiles to reveal the basement depths and fundamental resonance frequencies underneath three stations of Shillong plateau. The earthquake waveforms are recorded for a period of eighteen months (i.e. December 2018 to June 2020) using broadband seismometer; while the ambient microtremor data is collected from a three component highly sensitive velocity meter. The earthquake HVSRs and noise HVSRs are consistent with each other and range from ~3.6 Hz to ~14.5 Hz. The Rayleigh wave ellipticity are generated from the corresponding HVSR curves for inversion to determine compressional and shear wave velocity structure. We report that the compressional and shear wave velocity profiles match fairly well for both earthquakes and ambient microtremor data. Overall, Vs30 lies in the range of 480 m/s to 2600 m/s at all locations in the easternmost part of Shillong plateau; while the sedimentary layer velocity lies between 450 m/s and 1100 m/s. The thickness of the sedimentary layer is assessed from the velocity profiles and using an empirical formula makes a good match and varies from 11.3 m to 31.2 m.

INTRODUCTION

Northeastern India is an earthquake prone zone formed by the convergence of three tectonic plates viz. Indian plate, Burma plate and Eurasian plate. The region is also characterized by major geological features such as Shillong and Mikir plateau, Assam valley, Bengal basin and Mishmi hills. Historically, the region has suffered two great catastrophic earthquakes (M>8.0) – the 1897 Assam earthquake (Mw=8.7) and the 1950 great Assam-Tibet earthquake (Mw =8.6) – and several medium magnitude earthquakes, including, 1869 Cachar earthquake (Mw=7.4), 2011 Sikkim earthquake (Mw=6.9), 2016 Imphal earthquake (Mw=6.1) and a more recent Assam earthquake of April 28, 2021 (Mw=6.4) (Coudurier-Curveur et al. 2020). The 1897 Assam earthquake and 1950 Assam-Tibet earthquake have caused extensive damage killing a total of 3,042 lives and a total loss of $30 million (Tillotson 1951). The 1869 Cachar earthquake also claimed significant damage to government and public properties in Shillong city and Nongpoh. In Tura, apart from landslides, the material from the failed slope got accumulated, blocking the water way and forming the lakes; masonry houses on the other hand also suffered major earthquakes (Oldham 1882; Bilham 2008; Baro and Kumar 2015; Baro et al. 2018). The northeastern region is categorized in the highest seismic zone 'V' of India (BIS 2016). Thus, any industrial development in this area must be done in consideration with a serious seismic hazard study. Seismic site characterization is an important step in seismic hazard analysis to estimate elastic physical properties of near surface lithology. The near surface lithology may strongly escalate damage from earthquakes by increasing amplitude and duration of shaking, and by responding non-linearly to incident earthquake energy (e.g. Olsen 2000). Though invasive conventional methods such as borehole analysis can be availed; but a simple, non-invasive and cost effective method is often preferred. This study utilizes the non-invasive seismic site characterization method of horizontal-to-vertical spectral ratios (HVSR) for soil characterization in the eastern part of Shillong plateau. The HVSR method has proven its efficacy in numerous previous seismic hazard studies for estimation of resonance frequency and corresponding HVSR amplitude of the site under investigation (Nogoshi and Igarashi 1970; Nakamura 1989). Even though the noise HVSR provides a good estimation of the fundamental frequency of the site, there can be a disparity in the estimation of sediment layer thickness for the regions where there are no sharp impedance contrast between the sediment layer and bedrock. This may happen because the ambient noise attenuates highly due to dispersion in the unconsolidated sedimentary soil (Bignardi 2017; Martorana et al. 2018). In such cases, earthquake data can be availed for better estimation of the results. The Rayleigh wave ellipticity curves are also derived to demonstrate the peak of fundamental resonance frequency at each observation site (Fäh et al. 2001, 2003).

The prime objectives of this study are to generate the HVSR curves and estimate the fundamental frequency for both earthquake data and ambient noise data, develop the velocity profiles and infer the site characteristics for the three stations in Shillong plateau and a comparison study between the event and noise results. For this purpose, the authors deployed three broadband seismic stations to collect earthquake waveforms for a period of eighteen months (December 2018 to June 2020) at three locations of eastern part of Shillong plateau viz. Mawryngkneng, Khliehriat and Jowai. Also, the ambient noise data are collected at these locations for the processing and inversion of HVSR curves. The HVSR curves give the predominant frequency and the measure of velocity contrast between the top sedimentary layer and the substratum (Parolai et al. 2002).

GEOLOGY AND SEISMOTECTONICS OF STUDY AREA

The Shillong plateau, with a total area of 47614 km2, was evolved due to the continental collision of the Indian and Eurasian plates to the north and Indo-Burman oblique subduction to the east. The simultaneous collision and subduction on these sides may be credited for emergence of tectonically complex units across entire northeastern India. The plateau is clearly surrounded by several discontinuities and lineaments, namely, the oblique strike-slip Dawki fault in the south, Brahmaputra lineament to the north, Dhubri fault in the west and NW-SE trending Kopilli fault in the east. The Kopilli fault separates Shillong plateau from Mikir hills and is considered to be an anticipated source of future major earthquake (Kayal et al., 2006). The Dawki fault mark the boundary between Bengal basin/Surma valley of Bangladesh and Precambrian Shillong plateau. The study area is mainly consist of Shillong series of parametamorphites containing mostly sandstones and quartzites with relatively smaller amount of schist, phyllites, slates etc (Kalita 1998). The Shillong series rests upon conglomerate bed having cobbles and boulders of older rocks such as Archaean crystalline. These Shillong series rocks are considered to have been deposited probably in shallow marine conditions (Kalita, 1998). The "Khasi Greenstone" is prominently formed from the intrusion of Epidorite rocks which are mostly in the form of linear to curvilinear concordant and discordant Shillong group of metamorphosed rocks (Srinivasan et al., 1996). Generally, these rocks are extensively weathered substantially present within topographic depressions than in other areas.

PREVIOUS STUDIES IN THE REGION

Northeastern India has received a great deal of attention from geoscientists all across the world, especially for unraveling the regional and continental scale tectonics. These include seismic studies (Ramesh et al. 2005; Devi et al. 2009; Bora and Baruah. 2012a, b; Bora et al. 2014; Borah et al. 2016; Kumar et al. 2016; Raoof et al. 2017; Singh et al. 2017) as well as studies of gravity (Kayal and De, 1991; Khan and Chakraborty 2007; Nayak et al. 2008), geodesy (Mukul et al. 2010; Mahesh et al. 2012; Reddy et al. 2012), geodynamics (Duarah and Phukan 2011; Reddy et al. 2012; Vorobieva et al. 2017) and seismicity (Sukhija et al. 2006; Baro and Kumar, 2017). Although there are only a couple of studies dedicated to delineate the soil characteristics and ground response analysis in case of future earthquake scenarios. The site amplification study was accomplished using HVSR and generalized inversion technique for estimation of site amplification in Sikkim Himalaya (Nath et al. 2005). They also published a seismic microzonation hazard map prepared from thematic integration approach for the regions of Sikkim Himalaya and Guwahati city (Nath et al. 2008). Raghukanth and Somala (2009) derived the kappa factor (?0), quality factor (Q-value), stress drop and site amplification from strong motion data of the northeastern Indian region. The empirical relations between soil thickness and resonance frequency are developed for Shillong city to classify the sedimentary cover in the region(Biswas et al. 2015). Sharma et al. (2016) prepared ground motion response spectra obtained from earthquakes for various sites in northeastern India. They conclude that local site effects and regional geology has vital effect in the shape of acceleration response spectra. Baro et al. (2018) produced peak horizontal acceleration maps, via DSHA using suitable GMPEs, for three highly populated districts – the East Khasi hills, the Ri-Bhoi, and the West Garo hills – within the Shillong plateau. Their results indicate that the maximum spectral acceleration reaches 0.67 g, 0.77 g, and 0.64 g at 0.1s for the Shillong city, Nongpoh and Tura, respectively. Pandey et al. (2018) utilized HVSR curves generated from broadband earthquake seismograms recorded by twenty two stations, located sparsely all over northeastern India, installed by National Center for Seismology (NCS). Another study analyzed strong motion data of moderate size earthquakes recorded from twenty five locations of northeastern India. The recording sites were classified based on Vs30 and frequency of dominant peaks in the HVSR curve (Sandhu et al. 2020).

DATA AND METHODOLOGY

This study is carried out by collecting continuous ambient noise data from 'Tromino' manufactured by 'Micromed' and earthquake data from broadband seismic stations installed in the Shillong region for a period of 18 months starting from December 2018 at the locations of Mawryngkneng, Jowai and Khlieriat. The 'Trillium Compact 120s', a force balance three component seismometer manufactured by 'Nanometrics' connected to a centaur digitizer, is utilized for continuous earthquake data acquisition with 100 samples per second. On the other hand, microtremor data are collected using the "Tromino" made by

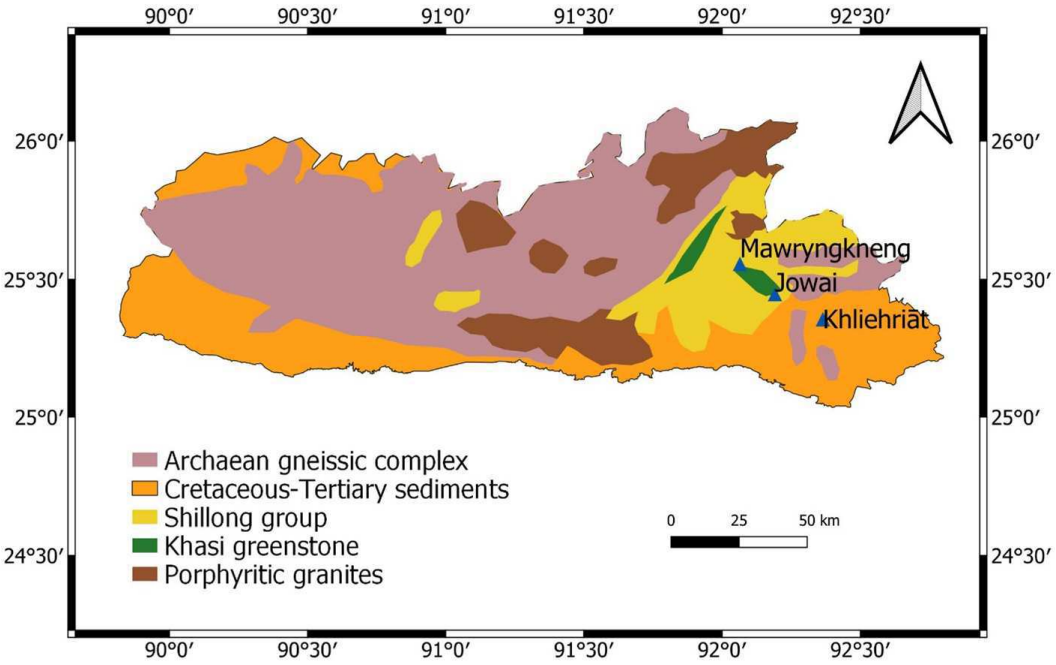

Fig. 1. Geological map of Shillong plateau with noise and event data recording sites marked in blue triangle.

"Micromed", which is equipped with a three component orthogonal electrodynamically highly sensitive velocity meters. The noise data are recorded by setting the 'Tromino' on the flat ground in the north-south direction with proper levelling as provided in manufacturer's instructions (Gupta et al. 2019, 2021).

The time window, mostly around S-wave arrival to surface wave's coda from ten regional earthquakes, are used to calculate the HVSR curves. On the other hand, 30 minutes of ambient noise records with sampling frequency of 1025 Hz are used for the estimation of noise HVSR as per the guidelines and recommendation of SESAME (2004). Then, the noise data is segmented into 20s stationary windows and triangular function is used for smoothening around 10% central frequency. All HVSR curves are generated for the frequency range between 0.4-30 Hz using open source portable software GEOPSY developed by Marc Wathelet (Wathelet et al. 2020). The GEOPSY software is used for the generation of HVSR curves and its extension GEOPSY-DINVER platform is employed for the inversion process.

The HVSR method was first proposed by Nogoshi and Igarashi (1970) and was further developed by Yutaka Nakamura (Nakamura 1989). This method is also known as Nakamura technique where the fundamental frequency and site amplification are estimated by calculating the horizontal to vertical amplitude spectrum of the microtremor or earthquake data. The HVSR is defined as the ratio of horizontal and vertical components of the amplitude spectra of a signal. The amplitude spectral components are generated by applying Fast Fourier Transform (FFT) and following mathematical relation is calculated to prepare HVSR curves.

$$\mathrm{HVSR} = \sqrt{((H^2_{(N\text{-}S)} + H^2_{(E\text{-}W)}) / V^2)} \quad (1)$$

where $H_{N\text{-}S}$, $H_{E\text{-}W}$ and V are the north-south, east-west and vertical amplitude spectral components of the waveform. The H/V tool in the GEOPSY is used to generate the HVSR curve. Before importing the signals, every three component dataset is cut into the desired time duration and every component is divided into small time windows to reduce the noise due to transient activities. An example of seismograms of event and noise with selected time windows are shown in Fig. 2. The Fourier transform of the signals are calculated to convert time series into the frequency domain. The resultant graph includes the averaged HVSR curve (black thick line), standard deviation (dashed lines) and the HVSR curves of individual time windows (coloured lines) (Fig. 3). The results also mark the fundamental frequency and corresponding H/V amplitude of the site (grey shade) (Fig. 3). The H/V amplitude depends not only on the source but also on the sediment type. The presence of unconsolidated sediments dominates the fundamental mode Rayleigh wave components in the frequency band above the resonant frequency which in turn affects the calculated H/V ratios. This ambiguity is minimized by extracting the ellipticity curve

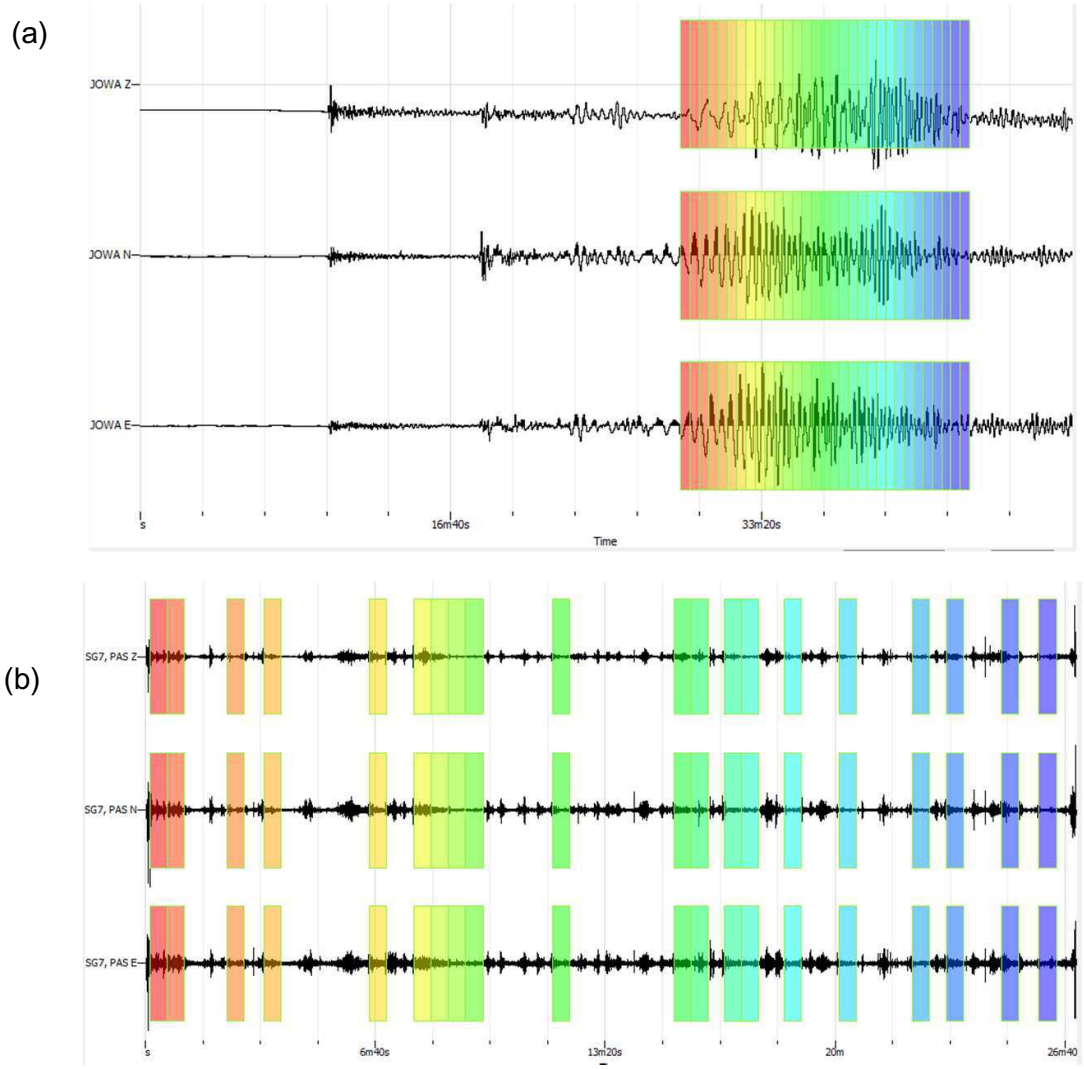

Fig. 2. The three component seismogram record of an earthquake **(a)** and microtremor **(b)** with time duration on x-axis and amplitude on y-axis. The Z, N and E denote the vertical, north-south and components, respectively. The color strips marks the constant time windows selected for HVSR curve generation.

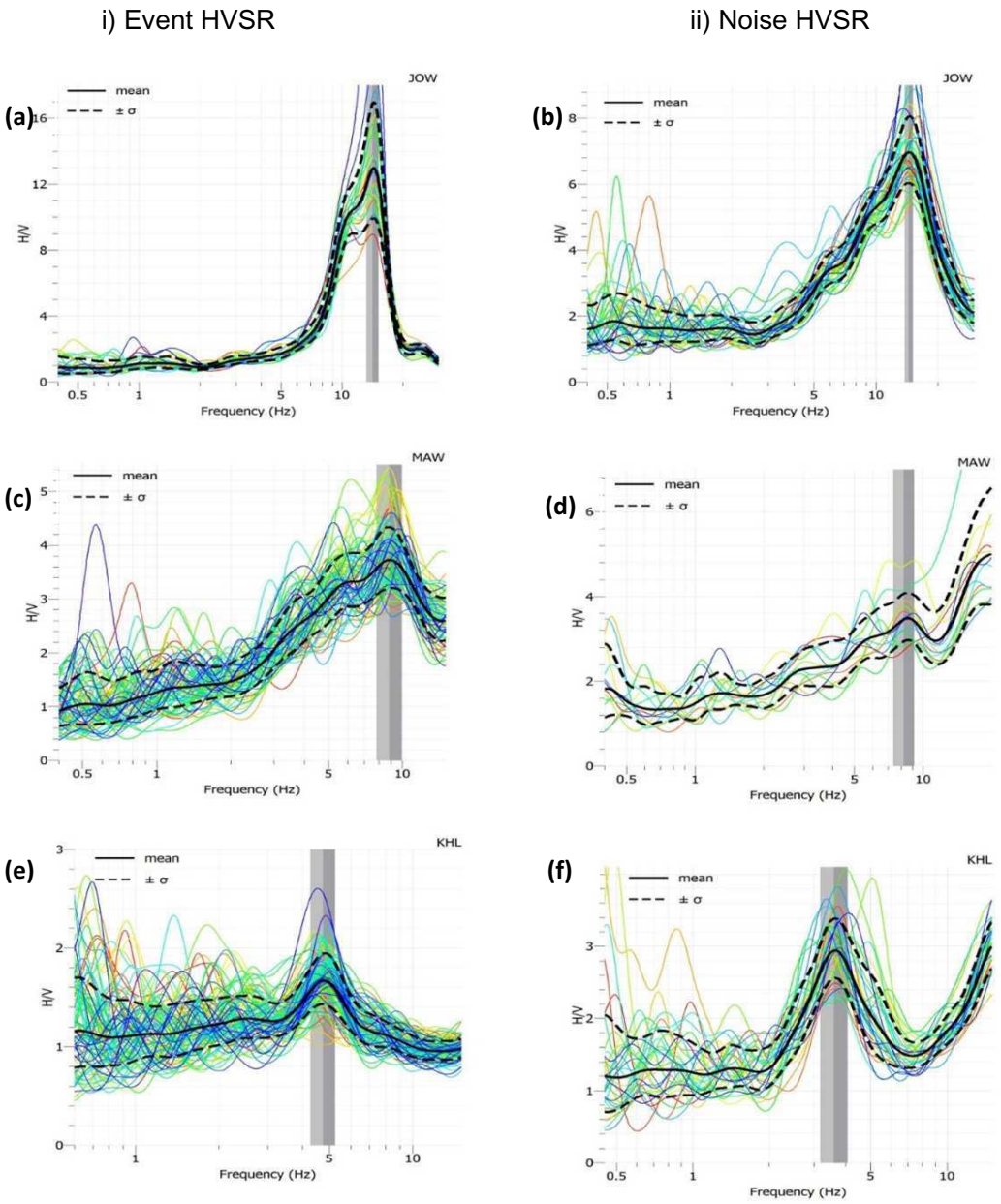

Fig. 3. HVSR curves for earthquake data (left panel) and ambient noise data (right panel) for Jowai (a,b), Mawrynkneng (c,d) and Khilehriat (e,f) stations. The colored lines indicate the HVSR curves for each individual time window with same color as that of the time window selected in the seismogram. The black thick line shows the averaged HVSR curve with dashed line representing the standard deviation added and subtracted. The grey region represents the range of fundamental frequency.

from the HVSR curve by applying frequency-time analysis and thereby optimizing the horizontal and vertical amplitude components in the signal (Fäh et al. 2001, 2003). For the calculation of ellipticity curve, the vertical components of the H/V spectra are scanned for a maxima. For each maximum observed on the time axis, corresponding horizontal spectral component is picked with a delay of one quarter of period, which is the theoretical delay for Rayleigh waves. The ratio of these horizontal to vertical values are noted for each maximum frequency. A histogram is prepared for each frequency with the log scale of the obtained ratio on the y-axis. The histogram will show a well-defined peak which corresponds to the ellipticity of that particular frequency (Fäh et al. 2009). The ellipticity curves obtained are inverted to get the velocity profiles of the study sites. Ellipticity targets are resampled for a frequency range near and above the fundamental frequency to obtain a better estimate of the shallow depth region. Four layer parameters viz. shear wave velocity, compression wave velocity, Poisson's ratio and density has to be given with desired number of layers by referring to priori information of the site. The inversion process is performed based on the neighborhood algorithm where the problem is approached by the random generation of samples from a parameter space and then Voronoi decomposition of parameter space is applied for the misfit value estimation (Sambridge 1999a, b). The final output will show the S wave velocity profiles including all those models with a lower misfit value. Integrating these individual velocity profiles, a 2D cross-section was generated along the line joining the location of stations.

Studies by Ibs-von Seht et al. (1999) have established an empirical relation using the fundamental frequency and the shear wave velocity as follows:

$$h = V_s / 4f \quad (2)$$

where h is the sediment layer thickness, V_s the shear wave velocity and f is the fundamental frequency. This empirical equation is applied

to estimate the sediment layer thickness of each site and the results are compared with those obtained from the velocity profiles.

RESULTS AND DISCUSSION

The objectives of this study are to compute the HVSR curves out of earthquake data and ambient noise data for three sites lying in the Shillong plateau, modelling the 1D velocity profiles by the inversion of these HVSR curves and finally a comparison study between event and noise results as well as between stations' results. The evaluated HVSR curves are shown in Fig.3 with earthquake HVSR (or eHVSR) in the left panel and ambient noise HVSR (or nHVSR) in the right panel. The standard deviations (or uncertainly) around the mean HVSRs (thick black lines) are shown in black dashed lines while the grey regions represent the range of fundamental frequency (Fig.3). The fundamental frequencies and fundamental amplitudes estimated from the plots (marked with grey color in Fig.3) are matched well for both event and noise data, except fundamental amplitude (A0) for JOW. The fundamental frequencies and amplitudes show substantial variation indicating heterogeneous subsurface material within the sub-surface beneath the easternmost part of Shillong plateau. The HVSR's from earthquakes and noise show variation from ~4.8 Hz to ~14.35 and ~3.6 Hz to ~14.5 Hz, respectively. The HVSR peaks are found to be very clear where the contrast between the overlying soft soil and the underlying bedrock is very high. However at Mawryngkneng (MAW), the nHVSR doesn't show a sharp peak while the eHVSR gives a relatively distinct peak (Figs. 3cd). The flat peak may present important information about the investigated area as the flatness is thought to arise from the weak impedance contrast between stiff sediments and the underlying hard bedrocks (Tun et al. 2016; Mahajan and Kumar 2018). The subsoil characteristics affect the distribution of noise components and thereby causing an uncertainty in the result, in such cases, earthquake HVSR may deliver additional information to validate the present findings from noise HVSR. Table 1 lists the fundamental frequencies and the H/V amplitudes obtained from the HVSR results. Figure 4 shows the averaged HVSR curves (left panel) and the corresponding ellipticity curves (right panel). Flat ellipticity peaks, similar to corresponding HVSR curves in Figure 3, for MAW station (Figs. 4c-d). This variation in the distribution of noise components may be due to the absence of sharp interfacial layers. The fundamental frequencies of nHVSR and eHVSR for KHL are shifted slightly and the same effect is noticed in the ellipticity curves as well (Figs. 4e-f). Such variations generally occur when a relatively lower value of resonant frequency is observed. The low resonant frequency corresponds to a higher depth interface. In such cases the surface waves attenuate in the unconsolidated sedimentary layer due to dispersion and scattering resulting in larger uncertainties. The conditions for obtaining a clear sharp peak is detailed in the article SESAME (2004). In each plot, the black and red colored curve indicate event and noise results respectively where frequency peak and curve shape of HVSR curves are retained precisely well in the ellipticity targets. These ellipticity targets are further used for the inversion purpose. Sharp peaks of fundamental frequency in the HVSR curves are an indication of strong impedance contrast between the overlying sedimentary layer and underlying bedrock. The sharp peak frequency in the HVSR curves of JOW station may have occurred because of the high impedance contrast aroused due to the high shear wave velocity of bedrock observed at the third layer of velocity profile (Figs. 5a-b). Figure 5 shows the 1D velocity profiles generated by the inversion of ellipticity curves. Both body wave and shear wave velocity profiles up to a depth of 40 m are shown in the figure separately for events (left panel) and noise (right panel). The colour band mentions the range of misfit values of the selected models. The lower the minimum misfit value more reliable the results will be. Figure 6 shows the 2D cross-section of the study site indicating shear wave velocity variations with depth which was produced by integrating the individual 1D shear wave velocity models of each station. Up to 40 m depth, three subsurface layers can be identified from the velocity profiles of all the stations. The lithology of these layers are estimated as soft sediments in the top layer, consolidated stiff sediments in the middle layer and bedrock in the bottom layer. While the interface between the first two layers lies at around 5 m depth for all the three stations, the sedimentary layer-bedrock interface extend between 22 m to 34 m from west to east. The layer boundaries of all stations matches reliably for both event and noise (Fig.5). From the velocity models the sedimentary layer thickness is measured to be around 16 m for both MAW and JOW station whereas that of KHL station is increased to about 27 m thickness. A comparison between sediment layer thickness obtained from inversion results and empirical formula is given in Table 2. Both the results complement well with each other. The sediment layer thickness lies in the range ~11.3 m to ~31.2 m with its value increasing from west towards east just like the trends shown in previous studies (Biswas et al. 2015). According to the study carried out by Biswas et al. (2015), the overburden sedimentary layer thicknesses are in agreement with the results presented in this paper. Since not much apriori information are available in this particular region, it is difficult to validate individual site results. The overburden

Table 1. Fundamental frequency and peak amplitude obtained from HVSR curves

Station	Data	F0 (Hz)	A0
JOW	Event	14.35	12.92
	Noise	14.53	6.96
MAW	Event	8.89	3.72
	Noise	8.59	3.45
KHL	Event	4.80	1.66
	Noise	3.63	2.94

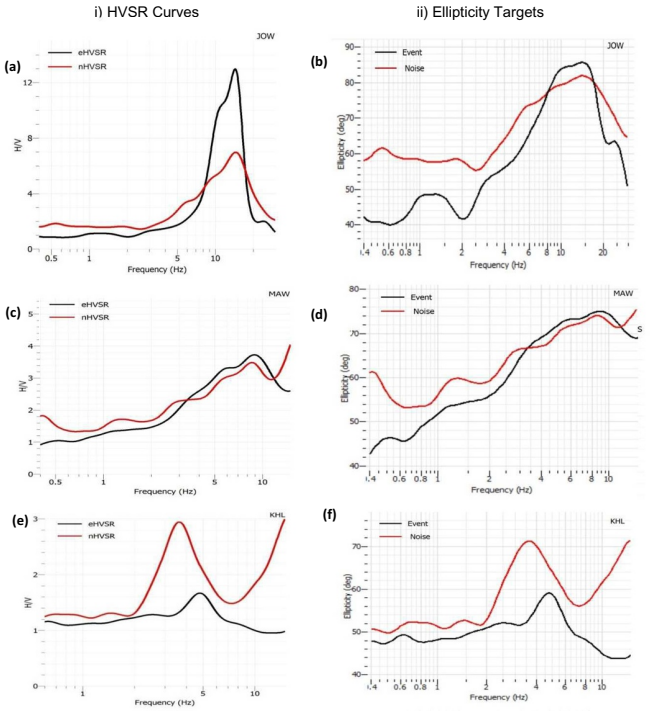

Fig. 4. Comparison of HVSR results (left panel) generated from noise data (red colored curve) and event data (black colored curve), and ellipticity targets (right panel) generated using the corresponding HVSR curves for Jowai (a,b), Mawrynkneng (c,d) and Khilehriat (e,f) stations.

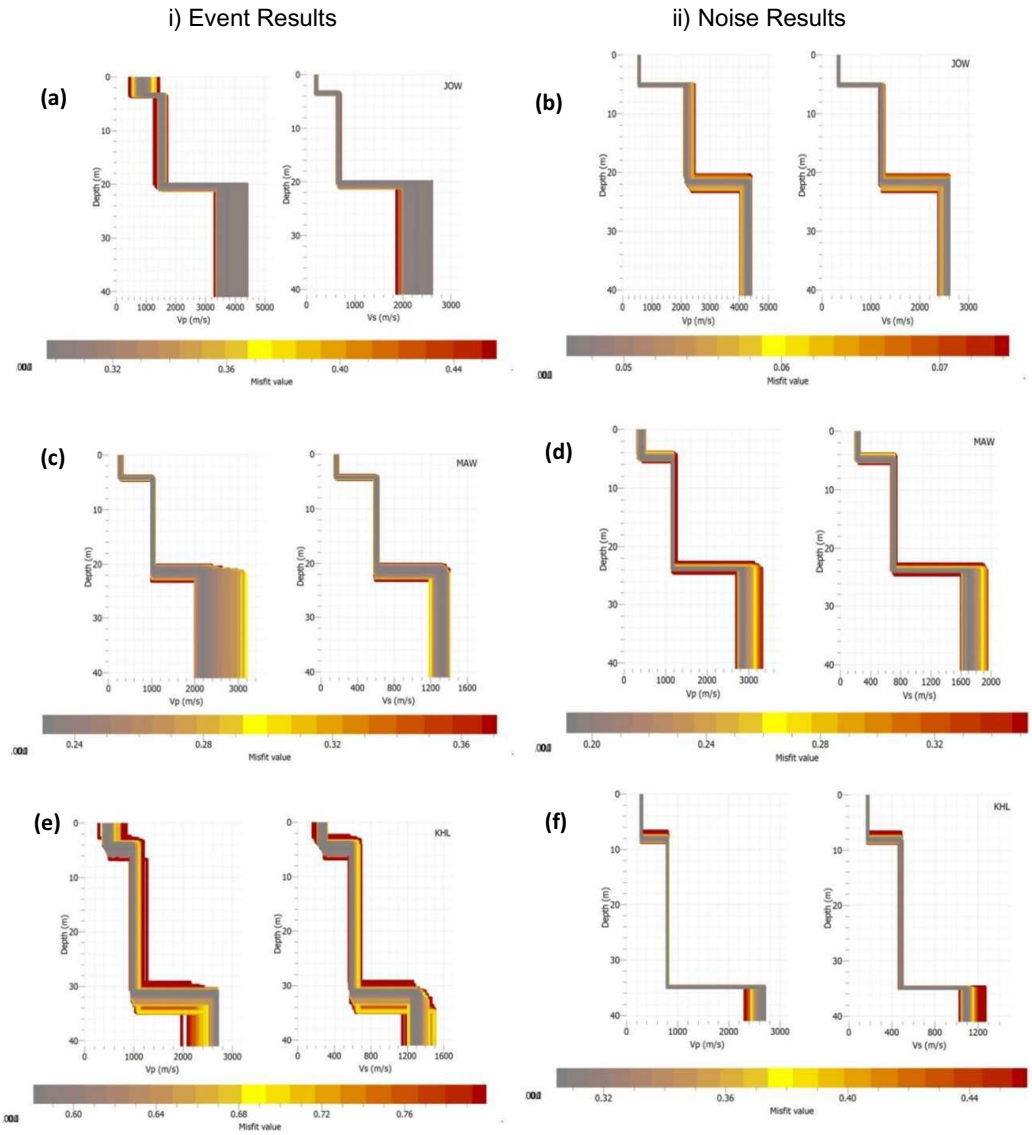

Fig. 5. Velocity profiles (up to 40 m depth) generated from the inversion of ellipticity curves of event data (left panel) and noise data (right panel) for Jowai (a,b), Mawryngkneng (c,d) and Khilehriat (e,f) stations. The color panel shows the misfit value range with grey region indicating models with minimum misfit.

loose sediments is having a shear wave velocity of 160 m/s to 380 m/s. Beyond that a sedimentary layer lies with shear wave velocity between 450 m/s to1100 m/s. This large velocity range is indicative of the presence of different types of sediments. The sediment type of Jowai and Khilehriat may be sandstone that is part of Surma Group and the sediment of Mawryngkneng may be quartzites of Shillong Group. The average shear wave velocity up to 30 m depth (i.e. Vs30) observed from inversion results of noise and event data are 2300 m/s and 2600 m/s for JOW, 1350 m/s and 1700 m/s for MAW and 600 m/s and 480 m/s for KHL, respectively. The lower Vs30 values at MAW are consistent with the quartzites of Shillong Group of rocks. The higher value of Vs30 attributes to the existence of old epidorite rocks known as "Khasi greenstone". According to NEHRP site classification based on Vs30, the soil profiles at each site will be, hard rock for JOW, firm to hard rock for MAW and dense soil or soft rock for KHL (Odum et al. 2007). Based on the NEHRP classification, KHL station is seismically more hazardous relative to the other two stations. As per the probabilistic hazard analysis (PHA) performed by Baro et al. (2018), the Eastern region of Shillong has a low peak horizontal acceleration (PHA) values of around 0.2 g which is consistent with NEHRP site classification. In the study carried out by Biswas et al. (2018), the shear wave velocity models generated for the Assam House station which is in the neighborhood of MAW station, appear to be consistent with this study results. Below 40m depth, two sub-surface layers are observed; one under 10m and the other around 30m for both Assam House and MAW stations where the shear wave velocity varies in the range of 200m/s to 700m/s.

Table 2. Comparison of sediment layer thickness obtained from inversion result and empirical formula

Station	Sediment layer thickness (m)	
	From velocity model	From empirical formula
JOW	15 - 19	11.3 - 19.2
MAW	16 - 20	15.5 - 19.7
KHL	23 - 29	23.4 - 31.2

CONCLUSIONS

In this study the HVSR curves and corresponding velocity profiles

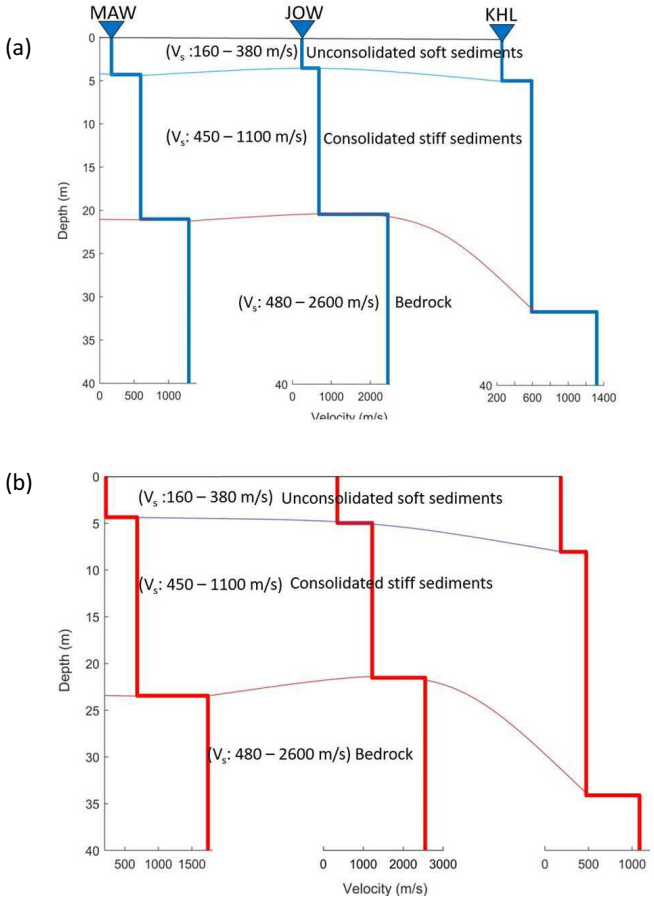

Fig. 6. 2-D cross-section (up to 40m depth) produced from the individual shear wave velocity models of event (a) and noise (b) Velocity range of each layer and corresponding soil type are indicated as well.

are generated from the earthquake and noise data for three broadband seismic stations in the eastern part of Shillong plateau. Both the event and noise data results are generally consistent with each other, which makes the results more reliable. The main conclusions of the conducted study are as follows:

- The fundamental frequency is observed to be different for each site with a westward decreasing trend where it ranges between ~3.6 Hz to ~14.5 Hz.
- Three sub-surface layers can be identified from the velocity profiles whose soil types are distinguished as unconsolidated soft sediments, consolidated sediment and bedrock from top to bottom.
- The lower fundamental frequency of around 4 Hz at Khliehriat is indicative of a thicker sedimentary layer of about 27 m obtained from the velocity profile.
- The sediment layer thickness for the entire study area lies in the range ~11.3 m to ~31.2 m with shear wave velocity between ~450 m/s to ~1100 m/s.
- The shear wave velocity at 30 m for all three stations covers a wider range of 480 m/s to 2600 m/s substantiating the prevalence of low velocity Shillong Group of quartzite to the oldest epidorite rocks having high velocity.

Acknowledgement: The authors acknowledge the support of the Head of the Department of Applied Geophysics for providing necessary infrastructure to successfully complete this study. Authors are grateful to associate editor, Dr. Prantik Mandal, and two anonymous reviewers for providing constructive comments which have eventually improved the quality of manuscript. The first author is also thankful to Prof. S.K. Pal who provided the support for 'Tromino'. All the departmental faculty members are thankfully acknowledged for their timely support during Covid-19 pandemic, which helped us significantly learn the complex concepts associated with this research. This research was funded by the Indian Department of Science and Technology (Project No. ECR/2016/001271 and SR/FST/ES-I/2017/12).

References

Baro, O. and Kumar, A. (2015) A review on the tectonic setting and seismic activity of the Shillong plateau in the light of past studies. Disaster Advances, v.8(7), pp.34-45.

Baro, O. and Kumar, A. (2017). Seismic source characterization for the Shillong Plateau in Northeast India. Jour. Seismol., v.21(5), pp.1229-1249.

Baro, O., Kumar, A. and Ismail-Zadeh, A. (2018). Seismic hazard assessment of the Shillong Plateau, India. Geomatics, Natural Hazards and Risk, v.9(1), pp.841-861.

Bignardi, S. (2017) The uncertainty of estimating the thickness of soft sediments with the HVSR method: A computational point of view on weak lateral variations. Jour. Appl. Geophys., v.145, pp.28-38.

Bilham, R. (2008) Tom La Touche and the great Assam earthquake of 12 June 1897: Letters from the epicenter. Seismol. Res. Lett., v.79(3), pp.426-437.

BIS (Bureau of Indian Standards). (2016). Indian standard criteria for earthquake resistant design of structures. IS 1893-16, New Delhi, India.

Biswas, R., Baruah, S. and Bora, D.K. (2015). Mapping sediment thickness in Shillong City of Northeast India through empirical relationship. Jour. Earthquakes, v.2015, Article ID 572619.

Biswas, R., Baruah, S. and Bora, N. (2018) Assessing shear wave velocity profiles using multiple passive techniques of Shillong region of northeast India. Natural Hazards, v.94(3), pp.1023-1041.

Bora, D.K. and Baruah, S. (2012a) Depth of mid-crustal discontinuity from reflected seismic waves on local earthquake seismograms recorded at Shillong Plateau, Northeast India. Geomatics, Natural Hazards and Risk, v.3(4), pp.355-364.

Bora, D.K. and Baruah, S. (2012b) Mapping the crustal thickness in Shillong-Mikir Hills Plateau and its adjoining region of northeastern India using Moho reflected waves. Jour. Asian Earth Sci., v.48, pp.83-92.

Bora, D.K., Hazarika, D., Borah, K., Rai, S.S. and Baruah, S. (2014) Crustal shear-wave velocity structure beneath northeast India from teleseismic receiver function analysis. Jour. Asian Earth Sci., v.90, pp.1-14.

Borah, K., Bora, D.K., Goyal, A. and Kumar, R. (2016) Crustal structure beneath northeast India inferred from receiver function modeling. Phys. Earth Plane. Inter., v.258, pp.15-27.

Coudurier-Curveur, A., Tapponnier, P., Okal, E., Van der Woerd, J., Kali, E., Choudhury, S., ... & Karaka, Ç. (2020). A composite rupture model for the great 1950 Assam earthquake across the cusp of the East Himalayan Syntaxis. Earth Planet. Sci. Lett., v.531, 115928.

Devi, E. U., Rao, N. P. and Kumar, M. R. (2009) Modelling of sPn phases for reliable estimation of focal depths in northeastern India. Curr. Sci., v.96, pp.1251-1255.

Duarah, B.P. and Phukan, S. (2011) Understanding the tectonic behaviour of the Shillong plateau, India using remote sensing data. Jour. Geol. Soc. India, v.77(2), pp.105-112.

Fäh, D., Kind, F. and Giardini, D. (2001) A theoretical investigation of average H/V ratios. Geophys. Jour. Internat., v.145(2), pp.535-549.

Fäh, D., Kind, F. and Giardini, D. (2003) Inversion of local S-wave velocity structures from average H/V ratios, and their use for the estimation of site-effects. Jour.f Seismol., v.7(4), pp.449-467.

Fäh, D., Wathelet, M., Kristekova, M., Havenith, H., Endrun, B., Stamm, G., ... and Cornou, C. (2009). Using ellipticity information for site characterisation. NERIES JRA4 "Geotechnical Site Characterisation". task B, 2.

Gupta, R.K., Agrawal, M., Pal, S.K. and Das, M. K. (2021). Seismic site characterization and site response study of Nirsa (India). Natural Hazards, doi:10.1007/s11069-021-04767-w.

Gupta, R.K., Agrawal, M., Pal, S.K., Kumar R. and Srivastava, S. (2019) Site characterization through combined analysis of seismic and electrical

resistivity data at a site of Dhanbad, Jharkhand, India. Environ. Earth Sci., v.78, pp.226. doi:10.1007/s12665-019-8231-2

Ibs-von Seht, M. and Wohlenberg, J. (1999) Microtremor measurements used to map thickness of soft sediments. Bull. Seismol. Soc. Amer., v.89(1), pp.250-259.

Kalita, B.C. (1998) Ground water prospects of Shillong Urban Aglomerate. Central Ground Water Board, Meghalaya (unpublished report).

Kayal, J.R. and De, R. (1991) Microseismicity and tectonics in northeast India. Bull. Seismol. Soc. Amer., v.81(1), pp.131-138.

Khan, P. K. and Chakraborty, P. P. (2007). The seismic b-value and its correlation with Bouguer gravity anomaly over the Shillong Plateau area: tectonic implications. Jour. Asian Earth Sci., v.29(1), pp.136-147.

Kumar, D., Reddy, D.V. and Pandey, A.K. (2016) Paleoseismic investigations in the Kopili fault zone of North East India: Evidences from liquefaction chronology. Tectonophysics, v.674, pp.65-75.

Mahajan, A.K. and Kumar, P. (2018) Site characterisation in Kangra Valley (NW Himalaya, India) by inversion of H/V spectral ratio from ambient noise measurements and its validation by multichannel analysis of surface waves technique. Near Surface Geophysics, v.16(3), pp.314-327.

Mahesh, P., Catherine, J.K., Gahalaut, V.K., Kundu, B., Ambikapathy, A., Bansal, A., ... and Kalita, S. (2012) Rigid Indian plate: constraints from GPS measurements. Gondwana Res., v.22(3-4), pp.1068-1072.

Martorana, R., Capizzi, P., D'Alessandro, A., Luzio, D., Di Stefano, P., Renda, P. and Zarcone, G. (2018) contribution of HVSR measures for seismic microzonation studies. Annals of Geophysics, v.61(2), SE225.

Mukul, M., Jade, S., Bhattacharyya, A.K. and Bhusan, K. (2010) Crustal shortening in convergent orogens: Insights from global positioning system (GPS) measurements in northeast India. Jour. Geol. Soc. India, v.75(1), pp.302-312.

Nakamura, Y. (1989) A method for dynamic characteristics estimation of subsurface using microtremor on the ground surface. Railway Technical Research Institute, Quarterly Reports, 30(1).

Nath, S.K., Thingbaijam, K.K.S. and Raj, A. (2008) Earthquake hazard in Northeast India-A seismic microzonation approach with typical case studies from Sikkim Himalaya and Guwahati city. Jour. Earth System Sci., v.117(2), pp.809-831.

Nath, S. K., Vyas, M., Pal, I. and Sengupta, P. (2005) A seismic hazard scenario in the Sikkim Himalaya from seismotectonics, spectral amplification, source parameterization, and spectral attenuation laws using strong motion seismometry. Jour. Geophys. Res.: Solid Earth, v.110(B1).

Nayak, G.K., Rao, V.K., Rambabu, H.V. and Kayal, J.R. (2008) Pop?up tectonics of the Shillong Plateau in the great 1897 earthquake (Ms 8.7): Insights from the gravity in conjunction with the recent seismological results. Tectonics, v.27(1), TC(1018). doi:10.1029/2006TC002027.

Nogoshi, M. and Igarashi, T. (1970) On the propagation characteristics of microtremors. Jour. Seism. Soc. Japan, v.23, pp.264-280.

Odum, J.K., Williams, R.A., Stephenson, W.J., Worley, D.M., von Hillebrandt-Andrade, C., Asencio, E., Irizarry, H. and Cameron, A., (2007) Near-surface shear wave velocity versus depth profiles, Vs 30, and NEHRP classifications for 27 sites in Puerto Rico. U. S. Geological Survey.

Oldham, T. (1882) A catalogue of Indian earthquakes from the earliest time to the end of A.D. 1869. Mem. Geol. Surv. India, v.19, pp.163-215.

Olsen, K.B. (2000) Site amplification in the Los Angeles basin from three-dimensional modeling of ground motion. Bull. Seismol. Soc. Amer., v.90(6B), pp.S77-S94.

Pandey, A.K., Roy, P.N.S., Baidya, P.R. and Gupta, A.K. (2018) Estimation of current seismic hazard using Nakamura technique for the Northeast India. Natural Hazards, v.93(2), pp.1013-1027.

Parolai, S., Bormann, P., & Milkereit, C. (2002) New relationships between Vs, thickness of sediments, and resonance frequency calculated by the H/V ratio of seismic noise for the Cologne area (Germany). Bull. Seismol. Soc. Amer., v.92(6), pp.2521-2527.

Raghukanth, S.T.G. and Nadh Somala, S. (2009) Modeling of strong-motion data in northeastern India: Q, stress drop, and site amplification. Bull. Seismol. Soc. Amer., v.99(2A), pp.705-725.

Ramesh, D.S., Ravi Kumar, M., Uma Devi, E., Solomon Raju, P., and Yuan, X. (2005) Moho geometry and upper mantle images of northeast India. Geophys. Res. Lett., v.32(14).

Raoof, J., Mukhopadhyay, S., Koulakov, I. and Kayal, J. R. (2017) 3?D seismic tomography of the lithosphere and its geodynamic implications beneath the northeast India region. Tectonics, v.36(5), pp.962-980.

Reddy, C., Sunil, P. S., Prajapati, S., Ponraj, M. and Amrithraj, S. (2011) Geodynamics of the NE Indian lithosphere: geodetic and seismotectonic perspective. Mem. Geol. Soc. India, no.77, pp.241-250.

Sambridge, M. (1999a) Geophysical inversion with a neighbourhood algorithm-I. Searching a parameter space. Geophys. Jour. Internat., v.138(2), pp.479-494.

Sambridge, M. (1999b) Geophysical inversion with a neighbourhood algorithm-II. Appraising the ensemble. Geophys. Jour. Internat., v.138(3), pp.727-746.

Sandhu, M., Sharma, B., Mittal, H., & Chingtham, P. (2020). Analysis of the site effects in the North East region of India using the recorded strong ground motions from moderate earthquakes. Jour. Earthquake Engg., pp.1-20.

SESAME. (2004) Guidelines for the implementation of the H/V spectral ratio technique on ambient vibrations-measurements, processing and interpretations, SESAME European research project EVG1-CT-2000-00026, deliverable D23.12. SESAME: Site EffectS Assessment Using AMbient Excitations, March, pp.1-62.

Sharma, B., Chopra, S., Chingtham, P. and Kumar, V. (2016) A study of characteristics of ground motion response spectra from earthquakes recorded in NE Himalayan region: an active plate boundary. Natural Hazards, v.84(3), pp.2195-2210.

Singh, A.P., Purnachandra Rao, N., Ravi Kumar, M., Hsieh, M. C. and Zhao, L. (2017) Role of the Kopili Fault in Deformation Tectonics of the Indo-Burmese Arc Inferred from the Rupture Process of the 3 January 2016 M w 6.7 Imphal Earthquake. Bull. Seismol. Soc. Amer., v.107(2), pp.1041-1047.

Srinivasan, P., Sen, S. and Bandopadhaya, P.C. (1996) Study of variation of Paleocene-Eocene sediments in the shield areas of Shillong Plateau. Rec. Geol. Surv. India, v.129(pt 4), pp.77-78.

Sukhija, B.S., Reddy, D.V., Kumar, D. and Nagabhushanam, P. (2006) Comment on "Interpreting the style of faulting and paleoseismicity associated with the 1897 Shillong, northeast India, earthquake: Implications for regional tectonism" by CP Rajendran et al. Tectonics, v.25(2).

Tillotson, E. (1951) The great Assam earthquake of August 15, 1950. Nature, v.167(4239), pp.128-130.

Tün, M., Pekkan, E., Özel, O. and Guney, Y. (2016) An investigation into the bedrock depth in the Eskisehir Quaternary Basin (Turkey) using the microtremor method. Geophys. Jour. Internat., v.207(1), pp.589-607.

Vorobieva, I., Mandal, P. and Gorshkov, A. (2017) Block-and-fault dynamics modelling of the Himalayan frontal arc: Implications for seismic cycle, slip deficit, and great earthquakes. Jour. Asian Earth Sci., v.148, pp.131-141.

Wathelet, M., Chatelain, J. L., Cornou, C., Giulio, G. D., Guillier, B., Ohrnberger, M. and Savvaidis, A. (2020) Geopsy: A user-friendly open-source tool set for ambient vibration processing. Seismol. Res. Lett., v.91(3), pp.1878-1889.